Published By Guangdong Pharmaceutical University, Guangzhou

Journal of Holistic Integrative Pharmacy

2022, 3(2): 147-160

EXPERIMENTAL RESEARCH

Isolation and characterization of water-soluble fractions of black sesame pigment and its antioxidant activities *in vitro*

WU Jihong[1], HUANG Qian[1], ZHU Shuang[1], SHAN Sharui[1], HU Jinmei[2], ARSHAD Mehmood Abbasi[3], ZHOU Lin[1*]

[1]*Guangdong Province Key Laboratory for Biotechnology Drug Candidates, School of Biosciences and Biopharmaceutics, Guangdong Pharmaceutical University, Guangzhou 510006, China;*

[2]*Department of Food Engineering, Guangdong Polytechnic of Environmental Protection Engineering, Foshan, 528216, China*

[3]*Department of Environmental Sciences, COMSATS Institute of Information Technology, Abbottabad 22060, Pakistan*

[Abstract] **Objective** Black sesame pigment (BSP) was a natural pigment with a variety of bioactivities, including antioxidant, antimutagenic, and neuroprotective properties. However, the high molecular weight and heterogeneous structure of BSP necessitate further investigation. The study's goal is to develop a theoretical foundation for water-soluble BSP as a potential functional food supplement. **Methods** First, crude black sesame pigment (rBSP) was extracted from black sesame by sodium hydroxide-hydrochloric acid method, furtherly two water-soluble components (BSP-1, BSP-2) were prepared from rBSP by the separation methods of macroporous adsorption resin. In the dynamic test, 40% ethanol (*v*/*v*) was applied to five different macroporous resins (AB-8, D101, XAD-1600, D201, and HPD-600) for static adsorption/desorption of rBSP separation. The structure of the components was investigated using ultraviolet (UV) spectroscopy, Fourier-transform infrared spectroscopy (FT-IR), and ^{1}H and ^{13}C nuclear magnetic resonance (NMR). Oxygen radical absorption capacity (ORAC) and cellular antioxidation activities (CAA) were used to assess the antioxidant activity of the components. **Results** A macroporous polymeric adsorbent method was developed to obtain water-soluble fractions of rBSP. For the static adsorption/desorption characteristics of rBSP, five types of macroporous resins (AB-8, D101, XAD-1600, D201, and HPD-600) were evaluated, and two fractions (BSP-1 and BSP-2) were isolated from rBSP by 40% ethanol (v/v) on D101 resin in the dynamic test. Furthermore, ultraviolet-visible spectroscopy, Fourier-transform infrared spectroscopy, ^{1}H and ^{13}C NMR revealed that BSP-1 and BSP-2 were macromolecule conjugate structures, with BSP-2 having higher aromaticity than BSP-1. ORAC and CAA results showed that rBSP, BSP-1, and BSP-2 had comparable antioxidant activities. The BSP-2 exhibited the highest CAA value of 1121.92 ± 54.45 μmol QE/100 g, DW. **Conclusion** This study suggests that water-soluble BSP fractions could be used as functional food supplements that benefit human health.

[Key words] Black sesame pigment; Isolation; Characterization; Antioxidant activity

[*Corresponding author] E-mail: zhoulin@gdpu.edu.cn.

1 Introduction

Melanin is a naturally occurring pigment found in both animals and plants. Melanin has attracted attention due to a wide range of biological activities, including antioxidant activity[1], UV-protection[2], anti-carcinogenic effect[3], antitumor activity[4], anti-inflammatory activity,[5] and liver protective effect[6]. As a result, melanin has a great deal of potential for use in the functional food, cosmetics, nutraceuticals, and pharmaceutical industries.

Sesame (*Sesamum indicum* L.) is a major oilseed crop grown primarily in tropical and subtropical regions around the world[7]. Sesame lignans, such as sesamol and sesamin, have been shown to have a variety of health-promoting activities, including antioxidant, antimutagenic, neuroprotective, and anti-inflammatory properties[8-10]. The antioxidant activity of black sesame seeds may be superior to that of white sesame seeds, which has attracted more interest in them[11-13].Our group has recently reported phytochemical profiles, antioxidant and antiproliferative activities of twelve varieties of black and white sesame seeds[12,14]. According to these studies, black sesame seeds outperform white sesame seeds as antioxidant supplements. Plant pigments, in addition to their role as natural colorants, have recently begun to be recognized as bioactive substances due to their potential health benefits[15]. Carotenoids, anthocyanins, and betacyanins are bioactive pigments, and including them in our daily diet may help us avoid diseases like hypertension, diabetes, cancer, and cardiovascular disorders[16-17]. The antioxidant activity of melanin was well recorded by the research[18-21]. While the potential activities of black sesame pigment (BSP) have been revealed, such as good antioxidant efficiency in the 2,2-diphenyl-1-picrylhydrazyl (DPPH) radical assay, heavy metals binding capacity, antitumor activity, and anti-amyloid aggregation activity[3,22-24]. However, most studies on BSP[25-28] are based on the overall water-insoluble pigment, with few reports on the structure characters and activities of the pigments from black sesame seeds, which may be related to the water insoluble and heterogeneity structure of melanin. Furthermore, some studies have found that water-soluble sesame extracts have high antioxidant activity[29-30]. Furthermore, water-soluble antioxidants are expected to have a significant impact because they aid water-insoluble antioxidants in protecting against ROS-induced oxidative damage[31].

Two water-soluble black sesame pigment components were separated using macroporous resin column chromatography in this study, and the structure and antioxidant capacity of the water-soluble components were investigated. The characteristics of BSP adsorption and desorption on five macroporous resins were investigated. The fractions were then characterized using ultraviolet-visible (UV-vis), Fourier-transform infrared spectroscopy (FT-IR), ^{1}H, and ^{13}C NMR spectroscopies. Furthermore, oxygen radical absorption capacity (ORAC) and cellular antioxidant activity (CAA) assays were used to determine the antioxidant activities of rBSP and its fractions (BSP-1, BSP-2).

2 Materials and methods

2.1 Materials and reagents

Black sesame seeds were purchased from Four Seasons of Zaozhuang Granary Co., Ltd. (Shandong, China). The samples were kept at room temperature in a desiccator until they were used. Daxinganling Lingonberry Boreal Biotech Co., Ltd. (Heilongjiang, China) provided the BSP standard. Quercetin, fluorescein disodium salt, 2,2'-azobis-amidinopropane (ABAP), dichlorofluorescein diacetate (DCFH-DA), and 6-hydroxy-2,5,7,8-tetramethylchronman-2-carboxylic acid (Trolox) were purchased from Sigma Chemical Co. (St. Louis, MO, USA). Gibco Life Technologies

Co. (Grand Island, NY, USA) provided Hank's balanced salt solution (HBSS), Williams' medium E, insulin, and other cell culture reagents. Deuterated dimethylsulfoxide (DMSO-d_6) and D_2O were purchased from Shanghai Macklin Biochemical Co., Ltd. (Shanghai, China). The resin AB-8 and D201 were purchased from Zhangzhou Baoen Adsorption Material Technology Co., Ltd. (Fujian, China). H&E Co., Ltd. (Beijing, China) provided the XAD-1600. D101 was purchased from NanKai University's Chemical Plant (Tianjing, China). Donghong Chemical Co., Ltd. (Jiangsu, China) supplied the HPD-600. All other reagents were of analytical grade and were obtained from Sangon Biotech Co., Ltd. (Shanghai, China).

2.2 Extraction of rBSP

The rBSP was extracted from black sesame seeds, as previously reported, with some modifications[3]. 50 g pulverized black sesame seed was treated with 750 mL freshly prepared 10 mg/mL sodium hydroxide solution while stirring, and then the mixture was shaken at 140 rpm for 40 min in a rotary rocker at 30 ℃. The suspension was then filtered through Whatman No. 5 filter paper, and the filtrate was centrifuged at 8 000 rpm for 10 minutes to remove insoluble impurities. The grease was removed from the separation funnel after 30 min of standing. The pH of the solution was adjusted to about 2.0 using a 1.5 M hydrochloric acid solution by stirring, and then centrifuged again. Finally, precipitates of rBSP were collected and dried to constant weight at 60 ℃.

2.3 Determination of rBSP content

The rBSP was dissolved in 0.05 M sodium bicarbonate to a final concentration of 0.10 mg/mL. To determine the maximum absorption wavelength, the samples were scanned with a UV-visible spectrophotometer (UV 550PC, Shanghai). The UV-vis spectroscopic method was used to determine the rBSP content of the extracts. The rBSP standard was dissolved in an aqueous solution of sodium bicarbonate (0.05 M) and ethanol (40% *v*/*v*). The samples were then examined with a UV-vis spectrophotometer to determine the maximum absorption wavelength (Fig. 1). Two standard curves were created for rBSP estimation at concentrations ranging from 0.0105 to 0.063 0 mg/mL in 0.05 M sodium bicarbonate and 0.0053 to 0.053 0 mg/mL in 40% ethanol aqueous solution, respectively (Fig. 2).

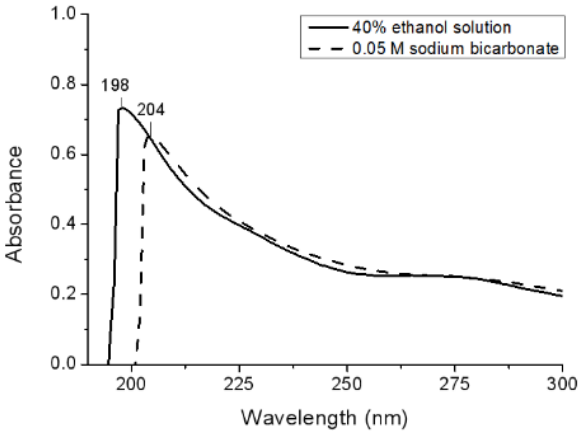

Fig. 1 UV-vis spectra of black sesame pigment standard in 0.05 M sodium bicarbonate and 40% (*v*/*v*) ethanol aqueous solution.

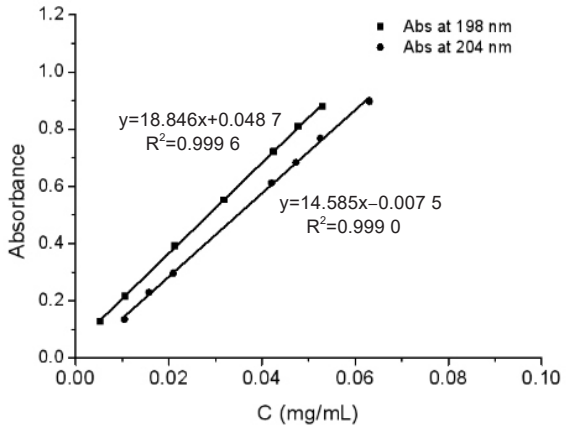

Fig. 2 The standard curve of black sesame pigment in 0.05 M sodium bicarbonate and in 40% (*v*/*v*) ethanol aqueous solution, at 204 nm and 198 nm, respectively.

2.4 Static adsorption and desorption tests

The resins' adsorption and desorption capacities were optimized. 20 mL rBSP solution was used to soak two grams of selected resins

(AB-8, D101, D201, HPD-600, and XAD-1600). To achieve adsorption equilibrium, the mixture was shaken at 120 rpm for 12 h at 25 ℃. The mixture was then filtered using Whatman No. 5 filtration paper, and the filtrate's absorption was measured at a maximum absorption wavelength of 204 nm.

The adsorption capacity of rBSP was calculated as follows:

$$Q_e=\frac{(C_0-C_e)\times V}{W_{wet}(1-\alpha)} \quad (1)$$

$$Q_{re}=\frac{(C_0-C_e)}{C_0}\times 100\% \quad (2)$$

Where C_0 and C_e denote the initial and equilibrium concentrations of rBSP in 0.05 M sodium bicarbonate solution (mg/mL), respectively; V denotes the volume of the initial sample solution (mL); W_{wet} denotes the weight of hydrated resins; α denotes the moisture content of the resins (%); Q_e denotes the equilibrium adsorption capacity (mg/g of dry resin); Q_{re} denotes the adsorption ratio (%).

The five adsorbed resins were filtered through Whatman No. 5 filter paper after reaching adsorption equilibrium. Following that, 40% ethanol was added to the resin in a liquid/solid ratio of 10∶1. To reach the desorption equilibrium, the mixture was shaken for 12 h at 120 rpm and 25 ℃. The filtrated solution was collected, and absorption at a maximum absorption wavelength of 198 nm was measured.

The desorption capacity of rBSP was quantified as the following equations:

$$Q_d=\frac{C_dV_d}{W_{wet}(1-\alpha)}\times 100\% \quad (3)$$

$$D=\frac{C_dV_d}{(C_0-C_e)V}\times 100\% \quad (4)$$

Where C_d denotes the concentration of rBSP in 40% ethanol after static desorption test (mg/mL); V_d denotes the volume of the desorption solution (mL); Q_d denotes the desorption capacity after desorption equilibrium (mg/g of dry resin); D denotes the desorption ratio (%). W_{wet}, α, V, C_0, and C_e denote the same as described as above. All tests were conducted in triplicates.

2.5 Optimization of the eluent

After reaching adsorption equilibrium, the D101 and HPD-600 resins were washed with deionized water. The adsorbed resins were then treated with a series of ethanol aqueous solutions (20%, 40%, 60%, and 80% (*v*/*v*), respectively) at a liquid/solid ratio of 10∶1. The mixture was then shaken (120 rpm) for 12 h at 25 ℃ before being filtered through Whatman No. 5 filtration paper. The filtrate was then dried at 50 ℃ until it reached a constant weight.

2.6 Dynamic adsorption/desorption experiments

In the dynamic experiments, glass columns (22 mm × 500 mm) were wet loaded by resins with a bed volume of 200 mL. The rBSP was dissolved in 250 mL of 0.05 M sodium bicarbonate (7.83 mg/mL) before being pumped through the resin column bed at a controlled flow rate of 1 mL/min. Following that, the sample-loaded resins were rinsed with 0.05 M $NaHCO_3$ and deionized water to remove impurities. Following that, at a rate of 2 mL/min, an ethanol-water (40%, *v*/*v*) solution was used. The separated fractions were identified using simultaneous ultraviolet-visible absorption spectrometry at 204 and 275 nm. Two fractions were lyophilized and kept at −20 ℃ until analysis.

2.7 Characterizations of rBSP and its fractions

The rBSP and its fractions (BSP-1 and BSP-2) were dissolved in sodium bicarbonate (0.05 M) to a final concentration of 1 mg/mL and their absorption properties were determined using UV-vis spectroscopy. The samples were diluted

with 0.05 M sodium bicarbonate solution and scanned at 190-600 nm, with the 0.05 M sodium bicarbonate solution serving as a control.

A Nicolet VERTEX 33 spectrometer (Bruker, Germany) was used to analyze the rBSP and its fractions using FT-IR at wave numbers 4 000-400 cm^{-1}. The ^{1}H and ^{13}C NMR spectroscopy spectrum was obtained at 25 ℃ using a 600 MHz Bruker AVANCEIII HD 600 spectrometer. BSP-1 and BSP-2 dissolved in DMSO-d_6 were detected at 600 MHz using ^{1}H NMR, while BSP-1 and BSP-2 dissolved in D_2O were detected at 151 MHz using ^{13}C NMR.

2.8 ORAC assay

The antioxidant activity of rBSP and its fractions (BSP-1, BSP-2) was measured using the ORAC assay, as previously reported[32]. In brief, 20 μL of phosphate buffer, Trolox standard, or rBSP solution were added to the appropriate well of a 96-cell plate and incubated for 10 min at 37 ℃. Following that, 200 μL of 0.96 μM fluorescein was added to each well and incubated at 37 ℃ for at least 20 min before starting the reaction with 20 μL of 119.4 mM ABAP. A fluorescent spectrophotometer was used to read the plate immediately at 485 nm of excitation and 535 nm of emission. The results are given in μmol Trolox equivalents per gram (mol Trolox equiv./g).

2.9 Cellular antioxidant activity (CAA) assay

The cellular antioxidant activity of rBSP and its fractions was determined using the CAA assay, as previously described[33]. HepG2 cells were seeded at 5.5×10^{4}/cells per well in a 96-well microplate with 100 μL of growth medium and incubated at 37 ℃. After 24 h, the medium was removed and washed with 100 μL of phosphate buffer solution (PBS). Individual cells received 100 μL of solution containing various concentrations of rBSP or quercetin solution plus DCFH-DA (50 M). After 1 h of incubation at 37 ℃, the medium was removed and washed with 100 μL PBS. The cells were then treated with 600 μM ABAP in 100 μL of HBSS, and the plate was read using a multi-mode microplate reader (Molecular Devices) at 485 nm excitation and 535 nm emission. CAA was expressed as μmol quercetin equivalents per 100 gram (μmol QE/100 g).

2.10 Statistical analysis

The data were presented as mean ± SD values. SPSS 22.0 was used to conduct the statistical analysis (IBM Corporation, New York, USA). The data were subjected to one-way analysis of variance, and the Tukey's multiple comparison test was used to assess differences between means. Statistical significance was defined as a *P*-value less than 0.05.

3 Results and discussion

3.1 Static adsorption and desorption capacities of tested resins

Table 1 shows the physico-chemical parameters of five types of resins used in the test. The skeleton material of all resins is styrene-divinylbenzene, but with varying polarities. The static adsorption and desorption capacities of rBSP

Table 1 Physical and chemical parameters of the tested resins

Trade name	Polarity	Particle diameter/mm	Surface area /(m^2•g^{-1})	Diameter average pore/nm	Moisture contents/%
AB-8	Weak-polar	0.30 - 1.25	480 - 520	12 - 16	65.83 ± 0.10
D101	Nonpolar	0.30 - 1.25	600 - 700	13 - 14	69.98 ± 0.15
XAD-1600	Nonpolar	0.35 - 0.45	800	15	72.82 ± 0.67
D201	Polar	0.32 - 1.25	330 - 380	-	52.31 ± 0.58
HPD-600	Polar	0.30 - 1.20	550 - 600	8	70.88 ± 0.09

on the tested resins are shown in Table 2. The adsorption capacities of HPD-600 are significantly higher (P<0.01) when compared to D201, but are comparable to D101 and XAD-1600. According to the "Similarly compatible" rule, HPD-600 had the highest adsorption ratios of 41.27% ± 2.51%, which could be attributed to the polarity of rBSP. D101 and XAD-1600 are nonpolar, with a larger adsorbent surface area and pore size than HPD-600, which could explain their high adsorption characteristics. This confirms that surface area as well as pore size were important factors in determining adsorption capacity. The results were comparable to anthocyanin separation[34-36]. In contrast to conventional nonpolar resins, anion exchange resins with broad adsorption behavior are designed for higher loading capacity and affinity toward target compounds, which can be tuned by adjusting the pH of the sample solution, which can be used as a reference in the subsequent research[37].

In static desorption tests, the desorption capacities of D101 and HPD-600 resins are significantly higher than those of D201 (P<0.01). However, the desorption ratio of HPD-600 is lower than that of D101, which may be due to its polarity. This indicates that polarity is one of the most important variables influencing the resin's desorption capacity. However, static tests revealed that HPD-600 and D101 were consistently more efficient at rBSP adsorption and desorption than other resins, and thus were used in further dynamic tests.

3.2 Determination of resin and elution solution

As shown in Fig. 3, the D101 resin had greater rBSP desorption capacity than the HPD-600 resin in the same ethanol aqueous solution concentrations (20%, 40%, 60%, and 80% (v/v), respectively), which could be attributed to their polarity. In general, the lower the polarity of the resin (D101), the lower the affinities between water-soluble components and adsorbent due to the rule "likes dissolve likes". Because of its ease of removal, recycling, low cost, and toxicity, ethanol is the preferred desorbent for macroporous resin[38]. Furthermore, because of its polarity, ethanol can be miscible with water, which may make it easier to separate water-soluble fractions of BSP. As a result, different concentrations of ethanol aqueous solutions (20%, 40%, 60%, and 80% (v/v), respectively) were used to perform desorption tests to find the best desorption solution and the optimal resin. As illustrated in Fig. 3, the desorption

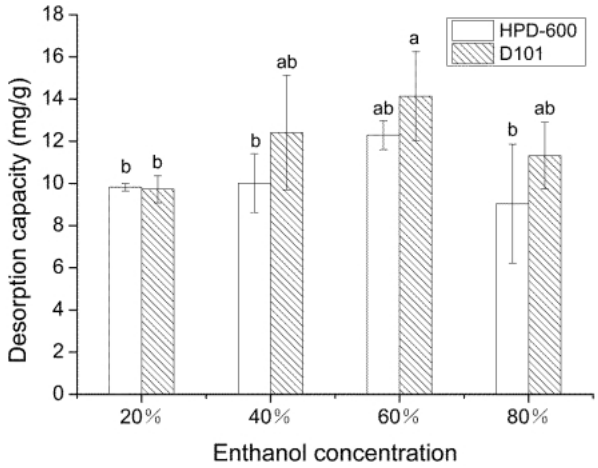

Fig. 3 Desorption capacity of the D101 and HPD-600 in different concentrations of ethanol aqueous ethanol solution 20%, 40%, 60% and 80% (v/v). Letters (a, b) indicate significant differences between groups and values with no letters in common are significantly different (P<0.05).

Table 2 Static adsorption and desorption capacities of rBSP on the five tested resins.

Type of resins	Q_e /(mg•g^{-1})	Q_{re}/%	Q_d/ (mg•g^{-1})	D/%
D101	12.92 ± 0.81**	32.52 ± 2.03*	11.69 ± 0.05**	90.71 ± 5.47**
HPD-600	16.91 ± 1.03**	41.27 ± 2.51**	10.15 ± 0.39**	60.11 ± 1.76**
XAD-1600	12.14 ± 0.92**	27.66 ± 2.10	8.83 ± 0.24**	73.00 ± 5.57**
D201	6.67 ± 0.41	26.67 ± 1.62	1.64 ± 0.06	24.62 ± 2.34
AB-8	7.42 ± 0.30	21.24 ± 0.86*	6.90 ± 0.30**	94.39 ± 2.38**

$^{**}P$<0.01, $^{*}P$<0.05 compared with D201 resin.

capacity of rBSP on HPD-600 and D101 increased with ethanol concentration, peaked at 60% ethanol, and then decreased at 80% concentration of ethanol aqueous solution. The different affinities of various rBSP components to the eluent can explain this result. Because hydrogen bonds are easily formed, the affinities between the water-soluble components and the ethanol aqueous solution were relatively stronger. The results were consistent with a previous report on anthocyanin purification using a macroporous resin[39]. It is worth noting that the ethanol-soluble components in rBSP were desorbed concurrently with the water-soluble components using a higher ethanol concentration, resulting in lower purity of the water-soluble components.

Furthermore, the 40% ethanol aqueous solutions had a slightly better desorption effect on two resins than the 60% ethanol aqueous solutions, ensuring that the water-soluble components were completely desorbed. However, there was no statistically significant difference (P>0.05) between the desorption capacities of two resins in 40% and 60% ethanol (Fig. 3). Because of the lower cost, 40% ethanol will be more suitable than 60% ethanol for large-scale industrial production. In summary, D101 resin and 40% ethanol aqueous solutions were chosen as the appropriate resin and desorption solvent for subsequent separation of the water-soluble rBSP fractions.

3.3 Dynamic adsorption/desorption assay

The rBSP fractions were eluted by a 40% ethanol solution, and the results are shown in Fig. 4. BSP-1 (78.30 mg) and BSP-2 (203.60 mg) fractions were obtained using UV-vis wavelengths of 204 nm and 275 nm, respectively. The BSP-2 elution peak was close to the BSP-1 elution peak. This result suggests that the difference between two fractions could be primarily due to structural differences in substitution groups or that they were isomers. Furthermore, we discovered that the two fractions are water soluble. In our preliminary work, we extracted a few components from rBSP using water. Water-soluble melanin, on the other hand, has been reported to be separated by resins[40-41]. As a result, we are trying to separate water-soluble fractions of rBSP from macroporous resins. The following structural analysis of two fractions would be useful in demonstrating their structural differences.

3.4 UV-vis spectrum analysis

The UV-vis spectrum of rBSP and its fractions is shown in Fig. 5, and that of rBSP standard is shown in Fig. 1. The maximum absorbance peaks of rBSP, BSP-1, and BSP-2 were 204 nm, 204 nm, and 203 nm, respectively, which was consistent with previous reports on melanin UV spectra[42]. Beyond 210 nm, the optical density of rBSP and

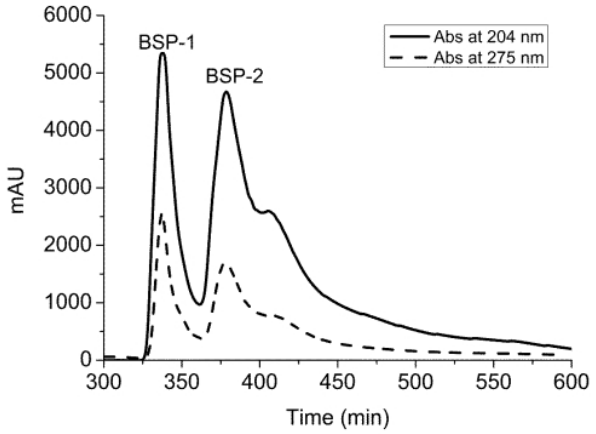

Fig. 4 Elution curve of rBSP separated on the D101 resin detected at 204 nm and 275 nm.

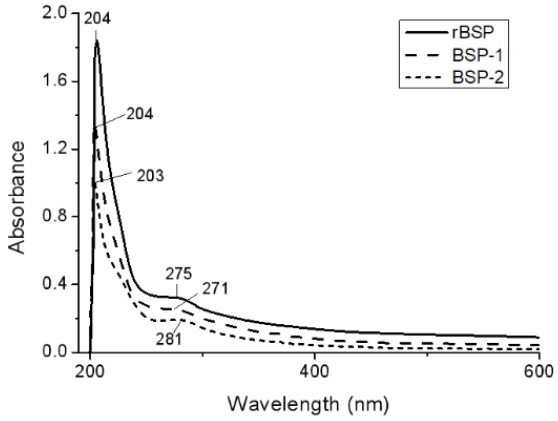

Fig. 5 UV-Vis spectra of rBSP, BSP-1 and BSP-2.

its fractions gradually decreased with increasing wavelength, which corresponded to melanin's typical UV radiation protection[43]. Furthermore, there was a typical small absorption peak in the 270-280 nm range, which could indicate the presence of conjugated structures in melanin[44]. Furthermore, a plot of log absorbance versus wavelength in the 400-600 nm range yields a linear curve with a negative slope, which is an important property of melanin[6]. Based on these findings, it is possible to conclude that BSP-1 and BSP-2 are melanin-like pigments.

3.5 FT-IR analysis

Fig. 6 depicts the FT-IR spectra of rBSP and its fractions (BSP-1 and BSP-2). The FT-IR spectra show strong similarities to previously studied BSP and melanin at typical infrared characteristic peaks[23,45-47]. The OH and NH stretching modes may be responsible for a strong and broad transmission peak between 3 500 cm^{-1} and 3 200 cm^{-1}. The two sharp peaks between 3 000 and 2 800 cm^{-1} confirm the presence of methyl and methylene groups. The aromatic C=C stretching was responsible for two strong transmission peaks in BSP-1 and BSP-2 between 1700 cm^{-1} and 1 500 cm^{-1}. Stretching vibrations of the groups C=O and C=C in melanin were observed at 1 650-1 600 cm^{-1}. Peaks in absorption between 1 500 cm^{-1} and 1 550 cm^{-1} corresponded to the bending vibration of N-H and the stretching vibration of C-N in melanin's nitrogen heterocyclic rings[48]. The phenolic OH is primarily responsible for the low-intensity bands between 1 400 cm^{-1} and 1 300 cm^{-1}. The region between 1 040 cm^{-1} and 1 243 cm^{-1} contains a variety of vibrations, including the C-N, C-O, C-O-C, and Ar-O bending. These findings suggest that rBSP, BSP-1, and BSP-2 are aromatic polymers. The weak peaks observed at 850-580 cm^{-1} suggest that some aromatic rings have been substituted with a small amount of aromatic hydrogen. The peaks of the two fractions have significant structural differences at 1 800-500 cm^{-1} when compared to the FT-IR spectum of rBSP (Fig. 6), which are primarily associated with the substitution pattern. BSP-1 has FT-IR spectum that are similar to BSP-2. However, at higher wave numbers, and peaks around 1 072 cm^{-1}, appeared to be weakened or even disappeared in BSP-2, indicating that some hydrogen bonds were replaced. BSP-2 has a weak absorption at 835 cm^{-1}, indicating that the aromatic C-H of BSP-2 contains more substitution than BSP-1. Peaks in 966-993 cm^{-1} correspond to aromatic C-H bonds, and their absence in the melanin spectra indicates that aromatic units are linked to each other in the pigments via C-C or C-O bonds[49].

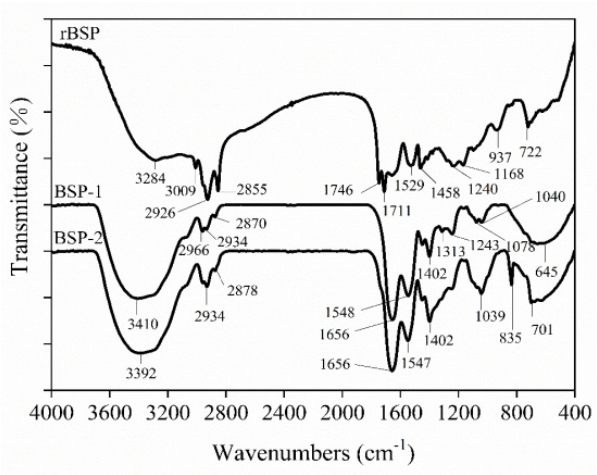

Fig. 6 FT-IR spectra of rBSP, BSP-1 and BSP-2.

3.6 NMR analysis

The composition of BSP-1 and BSP-2 was investigated further using ^{1}H NMR and ^{13}C NMR spectroscopy. The major signal regions of BSP-1 and BSP-2 are similar, as shown in Fig. 7. The major signal regions of ^{1}H NMR are as follows: 6.50-8.00 ppm, 3.00-5.00 ppm, and 0.80-2.00 ppm. Aromatic hydrogen of indole or pyrrole rings can be assigned to signals between 6.50 and 7.60 ppm[3]. A signal peak of OH on the ring may be present in the 8.27-9.00 ppm range. The broad peak around 8.00 ppm is attributed to protons bound to two aromatic rings[50]. Peaks in the absorption region from 3.00 to 5.00 ppm can

be assigned to protons on carbons attached to nitrogen and/or oxygen atoms[51]. Signals ranging from 0.80 to 2.00 are associated with methyl and methylene groups, such as methyl or the ester group of an aromatic ring. The signals at 3.66 ppm and 4.20 ppm could be from the OCH_3 and OH groups, respectively[52]. Peaks in the 4.00-5.00 range differ between BSP-1 and BSP-2, indicating a different aromatic nucleus with C=C–H[47]. The peaks of BSP-2 in this region (4.00-5.00 ppm) are stronger than those of BSP-1, implying that BSP-2 has higher aromaticity.

Fig. 8 depicts the ^{13}C-NMR spectra of BSP-1 and BSP-2. Both rBSP fractions have three signal regions in the 170-180 ppm, 125-135 ppm, and 0-50 ppm ranges. These signal regions indicate the presence of carbonyl, aliphatic, and aromatic functions[53]. BSP-2 was more intense in the aromatic region than BSP-1. The peak at 120-138 ppm is the signal peak caused by aromatic carbon. The resonance of a phenolic group caused a signal peak of 138-163 ppm[54]. Water-soluble pyridine is assigned to the strong resonance peak around 130 ppm[52]. Furthermore, the bands from 50 to 80 ppm differ significantly between BSP-1 and BSP-2. The signal peaks at 50-60 ppm in Fig. 8A were caused by carbon atoms in C-N or C-S groups[55], whereas the strong bands in Fig. 8B are related to the aromatic ring. These findings may point to the presence of more complex aromatic rings in the structure of BSP-2. In other words, BSP-2 is predicted to have a relatively high aromaticity, which is consistent with the FT-IR and ^{1}H NMR results. Furthermore, strong signal regions

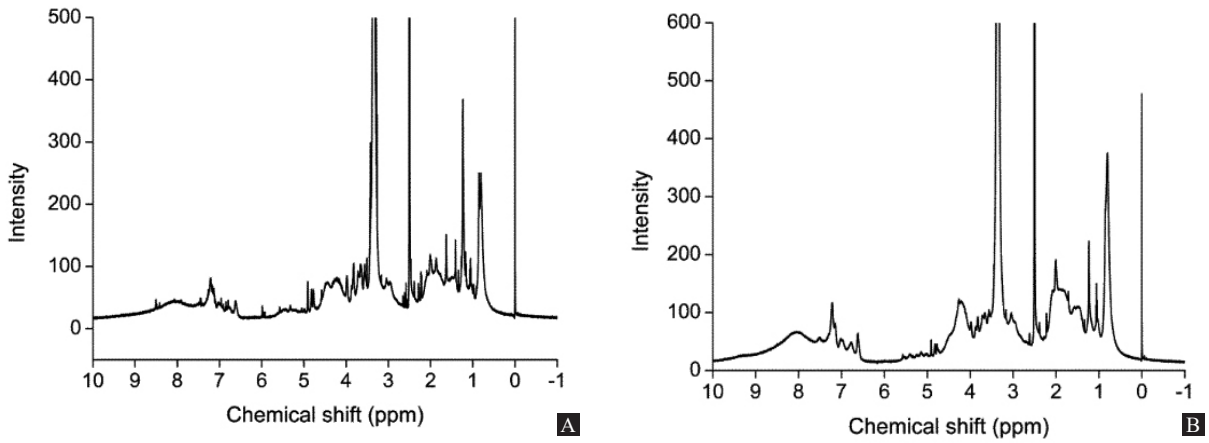

Fig. 7 ^{1}H NMR spectra of BSP-1 (A) and BSP-2 (B) (DMSO-d_6 as deuterated reagent and 600 MHz).

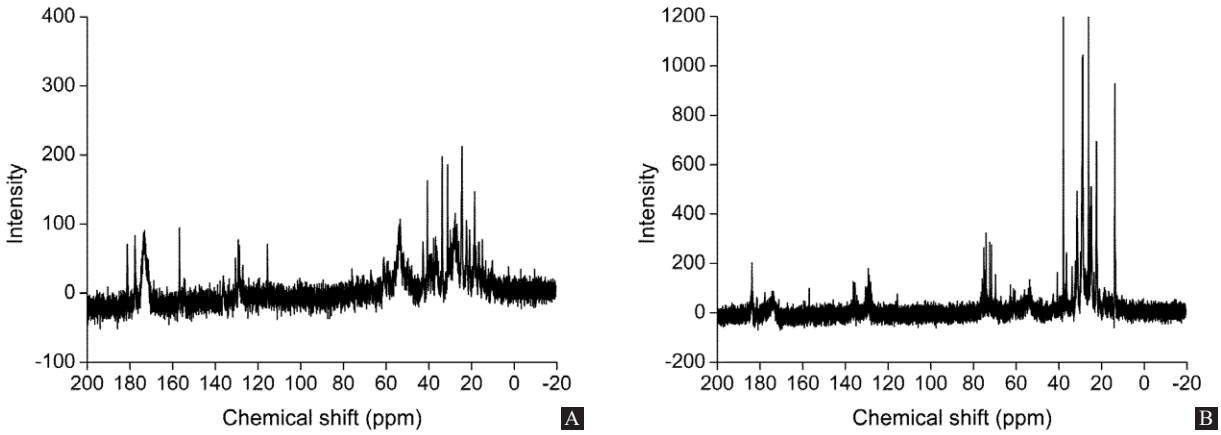

Fig. 8 ^{13}C NMR spectra of BSP-1 (A) and BSP-2 (B) (D_2O as deuterated reagent and 151 MHz).

in 170-180 ppm are mostly carboxyl carbons[56], implying that BSP-1 may have good UV-protection ability, which is consistent with melanin published in the literature[57].

3.7 Determination of total antioxidant activity

The ORAC assay has been widely used to assess the antioxidant activity of everyday foods against biologically relevant free radicals[58]. However, demonstrating the antioxidant activities *in vivo* is difficult. In comparison to expensive antioxidant methods based on animal models and human studies, the CAA assay is less expensive, takes less time, and is more suitable for antioxidant screening of foods[59]. As a result, ORAC and CAA assays were used to determine the total antioxidant activities of rBSP and its fractions.

The ORAC and CAA values of rBSP were 125.22 ± 4.42 μmol Trolox equiv./g, DW and 928.83 ± 16.21 μmol QE/100 g, DW, respectively, as shown in Table 3. In the current study, the value of ORAC was higher than that of oat (17.07-25.62 μmol Trolox equiv./g, DW) and blueberry (27.37-67.47 mol Trolox equiv./g, DW)[58,60]. However, rBSP had a lower ORAC value than Chinese hawthorn (398.3-555.8 mol Trolox equiv./g, DW)[61-62]. The CAA of BSP is significantly higher than that of antioxidant-rich foods (9.67-47 μmol QE/100 g, DW)[63]. The ORAC values of BSP-1 and BSP-2, on the other hand, were low, with values of 1.13 ± 0.03 and 0.94 ± 0.08 μmol Trolox equiv./g, DW, respectively. The ORAC values of rBSP were approximately 100-fold higher than those of its fractions, which could be attributed to the presence of additional antioxidant components in rBSP. Similar findings were discovered in the antioxidant activity of white sesame seed[14]. Currently, most studies on the ORAC values of natural pigments focus on curcumin and anthocyanin[64-66]. BSP had lower ORAC values than curcumin (14 981.34 ±298.41 μmol Trolox equiv./g, DW) and anthocyanin (11.44-17.88 μmol Trolox equiv./mg, DW)[67- 68].

Although the ORAC values of BSP-1 and BSP-2 did not differ significantly (P>0.05), the CAA assay revealed that BSP-2 had seven times the antioxidant activity of BSP-1. Furthermore, the aqueous solution of BSP-2 was dark brown, whereas the aqueous solution of BSP-1 was black. According to Xu et al, the brown pigment extracted by 75% (*v*/*v*) ethanol from black sesame seeds has the same antioxidant activity as BHA[69]. Although no structure information or CAA values were provided in Xu's study, it can be inferred that the brown BSP has a similar structure to BSP-2. Furthermore, the CAA value of BSP-2 was found to be 20% higher than that of rBSP, implying that BSP-2 may have more effective antioxidant properties. According to studies, the content of aromatic plant phenols is linearly positively correlated with antioxidant capacity[70], and other studies have shown that the total phenol content of fried tea leaves will increase, and the cellular antioxidant value can reach up to 1276 ± 38.29 μmol of QE/100 g DW[71], and the results of this experiment are consistent with related research. Panzella et al identified 4-hydroxy-3-methoxyphenyl motifs as the key structural moieties of BSP, and their levels in different pigment preparations were found to positively correlate with antioxidant properties[22]. Polyphenols derived from natural extracts have been shown in studies to have high antioxidant activity[72].

Table 3 ORAC and CAA values of rBSP and its fractions

	rBSP	BSP-1	BSP-2
ORAC values (μmol Trolox equiv./g DW)	125.22 ± 4.42	1.13 ± 0.03	0.94 ± 0.08
CAA values (μmol QE/100 g DW)	928.83 ± 16.21	166.35 ± 27.02	1 121.92 ± 54.45

As a result, BSP-2 may have a relatively high content of 4-hydroxy-3-methoxyphenyl motifs, leading to its high aromaticity. This hypothesis was supported by the previously mentioned FT-IR, ^{1}H, and ^{13}C NMR analyses, but further research is required. Several studies have used ORAC and CAA assays to determine the antioxidant activity of phenolic and flavonoid contents[29,58,63]. According to research, antioxidant activity has a relationship with its structure. It is also possible that ether-linked phenolic acids have a greater ferric reducing capacity than ester-bonded phenolic acids[73]. However, prior knowledge of the rBSP fraction was limited, and this work expanded our understanding of rBSP.

4 Conclusion

In conclusion, rBSP was prepared using dissolved alkali and acid precipitation, and two water-soluble fractions, BSP-1 and BSP-2, were separated using D101 resin and 40% ethanol elution. The UV-vis and FT-IR spectra of rBSP, BSP-1, and BSP-2 were comparable. The analysis of ^{1}H and ^{13}C NMR revealed that BSP-1 and BSP-2 were macromolecule conjugate structures, with BSP-2 having higher aromaticity than BSP-1. ORAC and CAA assay results showed that rBSP, BSP-1, and BSP-2 have high antioxidant activities, particularly the BSP-2 fraction. BSP-1 and BSP-2, in general, have a high potential for use as dietary antioxidants. This study shed light on how to separate and purify water-soluble antioxidant fractions from rBSP using macroporous resins. Further research into the mechanisms of antioxidant activities of rBSP fractions *in vivo* is suggested.

5 Abbreviations used

BSP black sesame pigment

rBSP crude black sesame pigment

BSP-1 water-soluble fraction one of black sesame pigment

BSP-2 water-soluble fraction two of black sesame pigment

FT-IR Fourier-Transform Infrared Spectroscopy

NMR Nuclear Magnetic Resonance

ORAC Oxygen Radical Absorbance Capacity

CAA Cellular Antioxidant Activity

6 Conflicts of Interest

These authors have no conflict of interest to declare.

7 Acknowledgement

This work was supported by the Guangdong Pharmaceutical University Research Cultivation Fund (43755008).

References

[1] Wu Z, Zhang M, Yang H, et al. Production, physico-chemical characterization, and antioxidant activity of natural melanin from submerged cultures of the mushroom *Auricularia auricula*[J]. *Food Biosci*, 2018, 26:49-56.

[2] Eskandari S, Etemadifar Z. Biocompatibility and radioprotection by newly characterized melanin pigment and its production from *Dietzia schimae* NM3 in optimized whey medium by response surface methodology[J]. *Ann Microbiol*, 2021, 71(1):17.

[3] Chu M, Hai W, Zhang Z, et al. Melanin nanoparticles derived from a homology of medicine and food for sentinel lymph node mapping and photothermal *in vivo* cancer therapy[J]. *Biomaterials*, 2016, 91: 182-199.

[4] Ye Z, Lu Y, Zong S, et al. Structure, molecular modification and anti-tumor activity of melanin from *Lachnum singerianum*[J]. *Process Biochem*, 2019, 76(JAN.):203-212.

[5] Wold CW, Gerwick WH, Wangensteen H, et al. Bioactive triterpenoids and water-soluble melanin from *Inonotus obliquus* (Chaga) with immunomodulatory activity[J]. *J Funct Foods*, 2020, 71:104025.

[6] Hou R, Liu X, Yan J, et al. Characterization of natural melanin from *Auricularia auricula* and its hepatoprotective effect on acute alcohol liver injury in mice[J]. *Food Funct*, 2019, 10(2):1017-1027.

[7] Wang L, Dossou SSK, Wei X, et al. Transcriptome dynamics during black and white sesame (*Sesamum indicum* L.) seed development and identification of

candidate genes associated with black pigmentation[J]. *Genes*, 2020, 11(12):1399.

[8] Andargie M, Vinas M, Rathgeb A, et al. Lignans of Sesame (*Sesamum indicum* L.): a comprehensive review[J]. *Molecules*, 2021, 26(4):883.

[9] Long H, Zhou C, Shi H, et al. Simultaneous HPLC quantification of four lignan glycosides in sesame seeds with the single reference standard method[J]. *Food Anal Methods*, 2020, 13(9):1774-1781.

[10] Yang Y, Wang J, Zhang Y, et al. Black sesame seeds ethanol extract ameliorates hepatic lipid accumulation, oxidative stress, and insulin resistance in fructose-induced nonalcoholic fatty liver disease[J]. *J Agric Food Chem*, 2018, 66(40):10458-10469.

[11] Agidew MG, Dubale AA, Atlabachew M, et al. Fatty acid composition, total phenolic contents and antioxidant activity of white and black sesame seed varieties from different localities of Ethiopia[J]. *Chem Biol echnol Agric*, 2021, 8(1):14.

[12] Zhou L, Lin X, Abbasi AM, et al. phytochemical contents and antioxidant and antiproliferative activities of selected black and white sesame seeds[J]. *BioMed Res Int*, 2016, 2016:8495630.

[13] Kim JH, Seo WD, Lee SK, et al. Comparative assessment of compositional components, antioxidant effects, and lignan extractions from Korean white and black sesame (*Sesamum indicum* L.) seeds for different crop years[J]. *J Funct Foods*, 2014, 7: 495-505.

[14] Lin X, Zhou L, Li T, et al. Phenolic content, antioxidant and antiproliferative activities of six varieties of white sesame seeds (*Sesamum indicum* L.)[J]. *RSC Adv*, 2017, 7(10):5751-5758.

[15] Luzardo-ocampo I, Ramirez-jimenez AK, Yanez J, et al. Technological applications of natural colorants in food systems: A review[J]. *FOODS*, 2021, 10(3):634.

[16] Fernandez-lopez JA, Fernandez-lledo V, Angosto JM. New insights into red plant pigments: more than just natural colorants[J]. *RSC Adv*, 2020, 10(41): 24669-24682.

[17] Hu YL, Luo JY, Hu SR, et al. Application of natural plant pigments in enlarged health industry[J]. Zhongguo Zhong yao za zhi, 2017, 42(13):2433-2438 (In Chinese).

[18] Cecchi T, Pezzella A, DI Mauro E, et al. On the antioxidant activity of eumelanin biopigments: a quantitative comparison between free radical scavenging and redox properties[J]. *Nat Prod Res*, 2020, 34(17):2465-2473.

[19] Liberti D, Alfieri ML, Monti DM, et al. A melanin-related phenolic polymer with potent photoprotective and antioxidant activities for Dermo-Cosmetic applications[J]. *Antioxidants*, 2020, 9(4):270.

[20] Di Mauro E, Camaggi M, Vandooren N, et al. Eumelanin for nature-inspired UV-absorption enhancement of plastics[J]. *Polym Int*, 2019, 68(5):984-991.

[21] Lin LC, Chen WT. The study of antioxidant effects in melanins extracted from various tissues of animals[J]. *Asian-Australas J Anim Sci*, 2005, 18(2):277-281.

[22] Panzella l, Eidenberger T, Napolitano A, et al. Black sesame pigment: DPPH assay-guided purification, antioxidant/antinitrosating properties, and identification of a degradative structural marker[J]. *J Agric Food Chem*, 2012, 60(36):8895-8901.

[23] Manini P, Panzella L, Eidenberger T, et al. Efficient binding of heavy metals by black sesame pigment: toward innovative dietary strategies to prevent bioaccumulation[J]. *J Agric Food Chem*, 2016, 64(4):890-897.

[24] Panzella L, Eidenberger T, Napolitano A. Anti-amyloid aggregation activity of black sesame pigment: toward a novel Alzheimer's disease preventive agent[J]. *Molecules*, 2018, 23(3):676.

[25] Xu J, Chen SB, Hu QH. Antioxidant activity of brown pigment and extracts from black sesame seed (*Sesamum indicum* L.)[J]. *Food Chem*, 2005, 91(1): 79-83.

[26] Mohdaly AAA, Smetanska I, Ramadan MF, et al. Antioxidant potential of sesame (*Sesamum indicum*) cake extract in stabilization of sunflower and soybean oils[J]. *Ind. Crops Prod*, 2011, 34(1):952-959.

[27] BaI L, Cheng X, Xu J, et al. Black sesame pigment extract from sesame dregs by subcritical CO_2: Extraction optimization, composition analysis, binding copper and antioxidant protection[J]. *LWT-Food Sci Technol*, 2019, 100:28-34.

[28] Nantarat N, Mueller M, Lin WC, et al. Sesaminol diglucoside isolated from black sesame seed cake and its antioxidant, anti-collagenase and anti-hyaluronidase activities[J]. *Food Biosci*, 2020, 36(2):100628.

[29] Othman SB, Katsuno N, Kanamaru Y, et al. Water-soluble extracts from defatted sesame seed flour show antioxidant activity *in vitro*[J]. *Food Chem*, 2015, 175:306-314.

[30] Bodoira R, Velez A, Andreatta AE, et al. Extraction of bioactive compounds from sesame (*Sesamum indicum* L.) defatted seeds using water and ethanol under sub-critical conditions[J]. *Food Chem*, 2017, 237(dec.15):114-120.

[31] Venkateswarlu S, Murty GN, Satyanarayana M, et al. Design, synthesis, and biological activity studies of a new class of sulfonated aurones: first synthesis of acidoaurone isolated from *phyllanthus acidus*[J]. *J Heterocycl Chem*, 2021, 58(12):2324-2333.

[32] Chen Y, Ma Y, Dong L, et al. Extrusion and fungal fermentation change the profile and antioxidant activity of free and bound phenolics in rice bran together with the phenolic bioaccessibility[J]. *LWT-Food Sci Technol*, 2019, 115:108461.

[33] Li CX, Zhao XH, Zuo WF, et al. Phytochemical profiles, antioxidant, and antiproliferative activities of red-fleshed apple as affected by *in vitro* digestion[J]. *J Food Sci*, 2020, 85(9):2952-2959.

[34] Chen Y, Zhang W, Zhao T, et al. Adsorption properties of macroporous adsorbent resins for separation of anthocyanins from mulberry[J]. *Food Chem*, 2016, 194(MAR.1):712-722.

[35] Xue H, Shen L, Wang X, et al. Isolation and purification of anthocyanin from blueberry using macroporous resin combined sephadex LH-20 techniques[J]. *Food Sci Technol Res*, 2019, 25(1): 29-38.

[36] Tao Y, Wu Y, Han Y, et al. Insight into mass transfer during ultrasound-enhanced adsorption/desorption of blueberry anthocyanins on macroporous resins by numerical simulation considering ultrasonic influence on resin properties[J]. *Chem. Eng J*, 2020, 380:122530-122536.

[37] Wang S, Zou R, Wu F, et al. HPLC-MS/MS analysis and study on the adsorption/desorption characteristics of ginsenosides on Anion-Exchange macroporous resins[J]. *Chromatographia*, 2021, 84(5):441-453.

[38] Jiang H, Li J, Chen L, et al. Adsorption and desorption of chlorogenic acid by macroporous adsorbent resins during extraction of *Eucommia ulmoides* leaves[J]. *Ind Crops Prod*, 2020, 149(122):336.

[39] Yao L, Zhang N, Wang C, et al. Highly selective separation and purification of anthocyanins from bilberry based on a macroporous polymeric adsorbent[J]. *J Agric Food Chem*, 2015, 63(13):3543-3550.

[40] Guo X, Chen S, Hu Y, et al. Preparation of water-soluble melanin from squid ink using ultrasound-assisted degradation and its anti-oxidant activity[J]. *J Food Sci Technol -Mysore*, 2014, 51(12):3680-3690.

[41] Wang LF, Rhim JW. Isolation and characterization of melanin from black garlic and sepia ink[J]. *LWT-Food Sci Technol*, 2019, 99:17-23.

[42] Al Khatib M, Costa J, Spinelli D, et al. Homogentisic acid and gentisic acid biosynthesized pyomelanin mimics: structural characterization and antioxidant activity[J]. *Int J Mol Sci*, 2021, 22(4):1739.

[43] Seelam SD, Agsar D, Halmuthur SKM, et al. Characterization and photoprotective potentiality of lime dwelling Pseudomonas mediated melanin as sunscreen agent against UV-B radiations[J]. *J Photochem Photobiol B*, 2021, 216:112126.

[44] Jalmi P, Bodke P, Wahidullah S, et al. The fungus *Gliocephalotrichum simplex* as a source of abundant, extracellular melanin for biotechnological applications[J]. *World J Microbiol& Biotechnol*, 2012, 28(2):505-512.

[45] Zhang MW, Sun L, Chi JW, et al. Comparative study on natural pigments in black rice, black soy bean and black sesame[J]. *J Chi Cer Oils Associ*, 1998, 13(2):6-9.

[46] Sun S, Zhang X, Sun S, et al. Production of natural melanin by *Auricularia auricula* and study on its molecular structure[J]. *Food Chem*, 2016, 190(80): 1-7.

[47] Zong S, Li L, Li J, et al. Structure characterization and lead detoxification effect of carboxymethylated melanin derived from *Lachnum sp.*[J]. *Appl Biochem Biotechnol*, 2017, 182(2):1-18.

[48] Xin C, Cheng C, Hou K, et al. A novel melanin complex displayed the affinity to HepG2 cell membrane and nucleus[J]. *Mat Sci Eng C-Mater*, 2021, 122(4):111923.

[49] Schmaler-ripcke J, Sugareva V, Gebhardt P, et al. Production of pyomelanin, a second type of melanin, via the tyrosine degradation pathway in *Aspergillus fumigatus*[J]. *Appl. Environ. Microbiol*, 2009, 75(2): 493-503.

[50] Bronze-uhle ES, Batagin-neto A, Xavier PHP, et al. Synthesis and characterization of melanin in DMSO[J]. *J Mol Struct,* 2013, 1047(1047):102-108.

[51] Katritzky AR, Akhmedov NG, Denisenko SN, et al. H-1 NMR spectroscopic characterization of solutions of Sepia melanin, Sepia melanin free acid and human hair melanin[J]. Pigm Cell Res, 2002, 15(2):93-97.

[52] Fulmer GR, Miller AJM, Sherden NH,et al. NMR chemical shifts of trace impurities: common laboratory solvents, organics, and gases in deuterated

solvents relevant to the organometallic chemist[J]. *Organometallics*, 2010, 29(9):2176-2179.

[53] Ye M, Guo GY, Lu Y, et al. Purification, structure and anti-radiation activity of melanin from *Lachnum* YM404[J]. *Int J Biol Macromol*, 2014, 63:170-176.

[54] Li S, Yang L, Li J, et al. Structure, molecular modification, and anti-radiation activity of melanin from lachnum YM156 on ultraviolet b-induced injury in mice[J]. *Appl Biochem Biotechnol*, 2019, 188(2): 555-567.

[55] Ye ZY, Lu Y, Zong S, et al. Structure, molecular modification and anti-tumor activity of melanin from *Lachnum singerianum*[J]. *Process Biochem*, 2019, 76(JAN.):203-212.

[56] Olennikov DN, Kirillina CS, Chirikova NK. Water-soluble melanoidin pigment as a new antioxidant component of fermented willowherb leaves (*Epilobium angustifolium*)[J]. *Antioxidants*, 2021, 10(8):1300.

[57] Riley PA. Melanin[J]. *Int J Biochem & Cell Biol*, 1997, 29(11):1235.

[58] Chen C, Wang L, Wang R, et al. Phenolic contents, cellular antioxidant activity and antiproliferative capacity of different varieties of oats[J]. *Food Chem*, 2018, 239:260-267.

[59] Liu RJ, Lu MY, Zhang T, et al. Evaluation of the antioxidant properties of micronutrients in different vegetable oils[J]. *Eur J Lipid Sci Technol*, 2020, 4(Supplement_2):446-446.

[60] Wang H, Guo X, Hu X, et al. Comparison of phytochemical profiles, antioxidant and cellular antioxidant activities of different varieties of blueberry (*Vaccinium* spp.)[J]. *Food Chem*, 2017, 217:773-781.

[61] Wen L, Guo X, Liu RH, et al. Phenolic contents and cellular antioxidant activity of Chinese hawthorn "*Crataegus pinnatifida*"[J]. *Food Chem*, 2015, 18(6):54-62.

[62] Ming WZ, Rui Z, Fang XZ. Phenolic profiles and antioxidant activity of black rice bran of different commercially available varieties[J]. *J Agric Food Chem*, 2010, 58(13):7580-7587.

[63] Wolfe K L, Liu RH. Cellular antioxidant activity (CAA) assay for assessing antioxidants, foods, and dietary supplements[J]. *J Agric & Food Chem*, 2007, 55(22):8896-8907.

[64] Pungcharoenkul K, Thongnopnua P. Effect of different curcuminoid supplement dosages on total in vivo antioxidant capacity and cholesterol levels of healthy human subjects[J]. Phytother Res, 2011, 25(11): 1721-1726.

[65] Wang Y, Zhu J, Meng X, et al. Comparison of polyphenol, anthocyanin and antioxidant capacity in four varieties of *Lonicera caerulea* berry extracts[J]. *Food Chem*, 2016, 197(APR.15PT.A):522-529.

[66] Fujita T, Sato-furukawa M, Sone K, et al. Effect of harvest time on changes in hydrophilic oxygen radical absorbance capacity of fruits from different strawberry cultivars (Fragaria X ananassa Duch.)[J]. *J Jpn Soc Food Sci*, 2020, 67(3):109-114.

[67] Choudhury AK, Raja S, Mahapatra S, et al.Synthesis and evaluation of the anti-oxidant capacity of curcumin glucuronides, the major curcumin metabolites[J]. *Antioxidants*, 2015, 4(4):750-767.

[68] Blando F, Calabriso N, Berland H, et al. Radical scavenging and anti-inflammatory activities of representative anthocyanin groupings from pigment-rich fruits and vegetables[J]. *Int. J Mol Sci*, 2018, 19(1):169.

[69] Xu J, Chen S, Hu Q. Antioxidant activity of brown pigment and extracts from black sesame seed (*Sesamum indicum* L.)[J]. *Food Chem*, 2005, 91(1): 79-83.

[70] Chiappero J, Del Rosario Cappellari L, Belen Palermo T, et al. A simple method to determine antioxidant status in aromatic plants subjected to drought stress[J]. *Biochem Mol Biol Educ*, 2021, 49(3):483-491.

[71] Chen YS, Shen YB, Fu X, et al. Stir-frying treatments affect the phenolics profiles and cellular antioxidant activity of *Adinandra nitida* tea (Shiyacha) in daily tea model[J]. *Int J Food Sci Technol*, 2017, 52(8): 1820-1827.

[72] Joly N, Souidi K, Depraetere D, et al. Potato by-products as a source of natural chlorogenic acids and phenolic compounds: extraction, characterization, and antioxidant capacity[J]. *Molecules*, 2021, 26:177.

[73] Connolly A, Cermeno M, Alashi AM, et al. Generation of phenolic-rich extracts from brewers' spent grain and characterisation of their *in vitro* and *in vivo* activities[J]. *Innovative Food Sci Emerging Technol*, 2021, 68(2):102617.